Diffusion of intrinsic localised modes by attractor hopping

Matthias Meister*†
Dpto. Física de la Materia Condensada
Facultad de Ciencias, Universidad de Zaragoza
50009 Zaragoza, Spain

and

Luis Vázquez‡
Dpto. Matemática Aplicada
Facultad de Informática, Universidad Complutense de Madrid
28040 Madrid, Spain

February 8, 2008

Abstract

Propagating intrinsic localised modes exist in the damped-driven discrete sine-Gordon chain as attractors of the dynamics. The equations of motion of the system are augmented with Gaussian white noise in order to model the effects of temperature on the system. The noise induces random transitions between attracting configurations corresponding to opposite signs of the propagation velocity of the mode, which leads to a diffusive motion of the excitation. The Heun method is used to numerically generate the stochastic time-evolution of the configuration. We also present a theoretical model for the diffusion which contains two parameters, a transition probability Θ and a delay time τ_A. The mean value and the variance of the position of the intrinsic localised mode, obtained from simulations, can be fitted well with the predictions of our model, Θ and τ_A being used as parameters in the fit. After a transition period following the switching on of the noise, the variance shows a linear behaviour as a function of time and the mean value remains constant. An increase in the strength of the noise lowers the variance, leads to an increase in Θ, a decrease in τ_A and reduces the finite average distance a mode travels during the transition period.

1 Introduction

Intrinsic localised modes (ILMs) are localised excitations that can occur in a system due to the interplay of discreteness and nonlinearity, for instance see [1]. These modes exhibit internal dynamics, like oscillations or rotations of constituents of the system in the localisation region. Therefore, these modes also are known as discrete breathers, alluding to the superficial similarity between them and the breather solutions of the continuum sine-Gordon equation. The majority of the literature deals with strictly time-periodic, non-propagating ILMs. For this specific type of discrete breather there are rigorous proofs of existence for the conservative [2, 3] and dissipative [4] cases. From the proofs it is clear that the requirements for the existence of these modes are rather

*email: matthias@unizar.es
†also at: Instituto de Biocomputación y Física de Sistemas Complejos, Universidad de Zaragoza, 50009 Zaragoza, Spain
‡also at: Centro de Astrobiología (CSIC-INTA), 28850 Torrejón de Ardoz, Spain

weak, which makes ILMs quite generic, in contrast to breather solutions in the continuum. An overview of some recent results can be found in [5].
First predictions [6] of the existence of such modes, however, did not exclude the case of propagating discrete breathers and numerical results [7] soon showed the existence of mobile ILMs. Several aspects of such travelling modes have been investigated so far, for example the interaction with an impurity [8] or the effects of a bending of the chain along which the excitation is travelling in connection with models of DNA [9, 10]. To our knowledge, the diffusion of intrinsic localised modes has not been looked at yet; this is in stark contrast to the thoroughly investigated topic of soliton / solitary wave diffusion. For the latter, see for instance [11–16] and references therein.
We study this problem in the discrete sine-Gordon chain (also known as the standard Frenkel-Kontorova model) under damping and harmonic driving; the equations of motion, in dimensionless units, are:

$$\frac{\mathrm{d}^2 u_n}{\mathrm{d}t^2} = -\frac{1}{2\pi}\sin(2\pi u_n) + C(u_{n+1} + u_{n-1} - 2u_n) - \alpha\frac{\mathrm{d}u_n}{\mathrm{d}t} + F\sin(\omega_0 t). \tag{1}$$

This equation describes the dynamics of a chain of identical damped and driven pendula in a homogeneous gravitational field, with harmonic nearest neighbour coupling. The quantity u_n corresponds to the angle of deviation (in units of 2π) of the n-th pendulum from the position of minimum energy. Certain systems of Josephson junctions can also be described by equation (1), see [17] for example.
Numerical results [18] show that intrinsically localised modes exist as attractors of the dynamics governed by this equation. In particular, within certain ranges of the parameters C, α, ω_0 and F the attracting configurations are propagating ILMs with well defined propagation velocities, dependent on the system parameters; apart from the fact that the discrete sine-Gordon equation is well-known, this has been the main motivation for our choice of equation (1). Due to the symmetry in the equations of motion, for each absolute value of the velocity we can have positive and negative sign, i.e. propagation to the right or left, respectively. There exist regions in parameter space where more than one absolute value of the propagation velocity v is possible at fixed parameters.
In order to model temperature we add Gaussian white noise terms $\xi_n(t)$ of strength σ, i.e.

$$\begin{aligned} \langle \xi_n(t) \rangle &= 0 \\ \langle \xi_m(t)\xi_n(t') \rangle &= \sigma^2 \delta_{mn}\delta(t-t') \end{aligned} \tag{2}$$

to the equations of motion (1) for the individual pendula. Such noise terms can be described in a clearer way by Wiener processes [19], but as the theoretical treatment of the diffusive motion we present in sections 3 and 4 does not make use of the formalism of stochastic differential equations, we do not tarry here. The relation between σ and the temperature T is $\sigma^2 = 2\alpha k_B T$, where k_B is Boltzmann's constant. It turns out that the noise causes random transitions between basins of attraction corresponding to opposite signs of the propagation velocity of the discrete breather, which brings about the diffusive motion of the excitation.
In section 2 we present all our numerical results, including the comparison with predictions to be derived in the next two sections. Section 3 discusses a theoretical model

for the diffusive behaviour of the modes which uses only the transition probability Θ between basins of attraction as a parameter; it is then improved in section 4 by the introduction of the delay time τ_A as a second parameter. We discuss the results and draw some conclusions in section 5. An appendix lists some intermediate results related to section 4.

2 Numerical Results

The simulations are done in a chain of 1000 particles with periodic boundary conditions (i.e. a ring). The stochastic time evolution according to (1) with the noise terms added is generated by the Heun algorithm (time step $\Delta t = 0.01$). We use parameter values $\alpha = 0.02, F = 0.02, \omega_0 = 0.2\pi$ and $C = 0.890$ along with several values of σ. The local energies

$$E_n = \frac{1}{2}p_n^2 + \frac{1}{(2\pi)^2}\left[1 - \cos(2\pi u_n)\right] \tag{3}$$

are used to define the position X of the localised mode as

$$X = \frac{\sum_{n=-2}^{n=+2}(n_0+n)E_{n_0+n}}{\sum_{n=-2}^{n=+2}E_{n_0+n}} \tag{4}$$

where the site n_0 is chosen in the following way: The distribution of the E_n sharply peaks around the location of the ILM. Usually, this peak has only one maximum. In this case, n_0 is the site where this maximum occurs. Sometimes, the peak displays a structure maximum-minimum-maximum on three subsequent sites. In this case n_0 is the site of the peak's minimum. Using (4) we calculate the position of the excitation out of the numerically generated configurations. Averaging over 500 realisations, we obtain the time evolution of the mean value of X as well as the variance of the position. In figure 1 we show some sample trajectories. We can see that the noise causes the system to jump between attracting states corresponding to opposite signs of the propagation velocity v. At the parameter values chosen, the system is known [18] to allow for at least two values of $|v|$, which are approximately 0.0186 and roughly twice that. As the trajectories shown already hint and a closer quantitative look confirms, only the former of the two values is involved. We cannot *strictly* exclude the appearance of more than just this one value of $|v|$, but our numerical results show that if this happens, it is a rare event. Transitions $v \approx 0.0186 \leftrightarrow v \approx -0.0186$ are clearly dominant. A comparison between the results from simulations and the predictions of the model in section 4 is shown in figure 2. We observe that the mean value approaches a σ-dependent value constant in time, i.e. after a transient there is no mean drift in the system. The variance, also after a transient, depends linearly on time, which is the result expected for standard diffusion (Brownian motion). Completely non-standard, however, is the fact that the diffusion constant, i.e. the slope of the variance as a function of time, decreases with increasing noise strength, i.e. increasing temperature. Such a temperature dependence has been reported for one of several diffusive processes contributing to the diffusion of kinks in a ϕ^4-model [13]. As we can see from figure 2, the theoretical model developed in sections

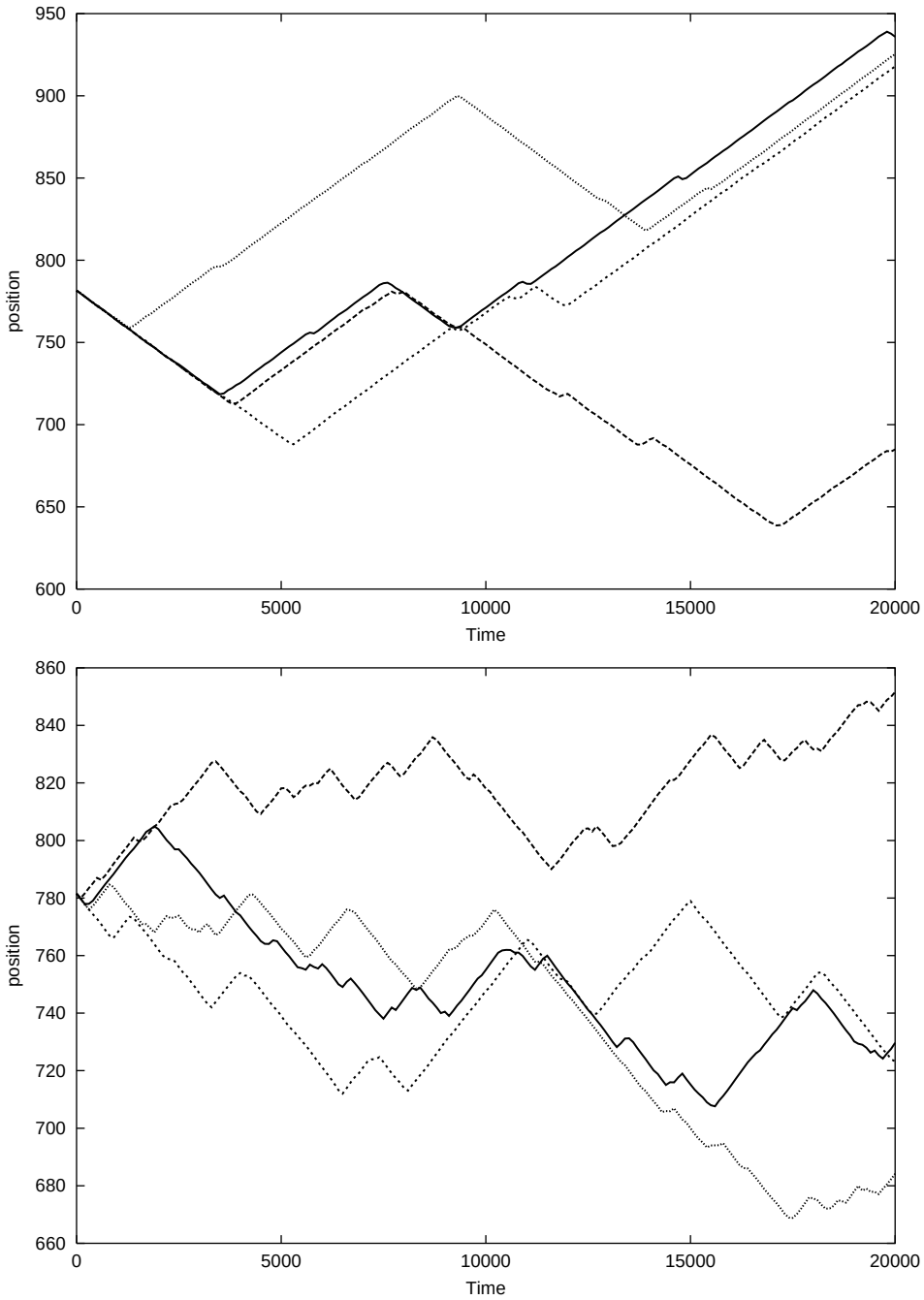

Figure 1: Some sample trajectories for two different strenghts of the noise. Top: $\sigma = 7 \cdot 10^{-5}$, Bottom: $\sigma = 12 \cdot 10^{-5}$. The position of the localised mode has been calculated every 100 time units.

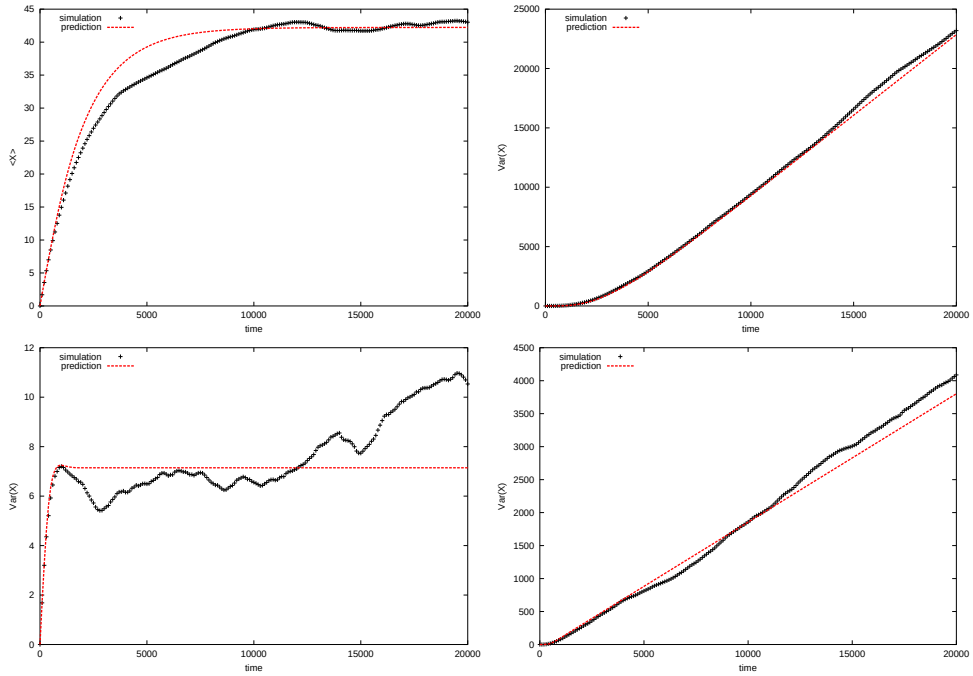

Figure 2: Comparison between data from simulations and results from the model of section 4. The simulation data are averages over 500 realisations. Left: Mean value of the position (with respect to the initial position), right: variance of the position. Top: $\sigma = 7 \cdot 10^{-5}$ (fitted parameters: $\Theta = 2.2 \cdot 10^{-4}, \tau_A = 700$), bottom: $\sigma = 12 \cdot 10^{-5}$ (fitted parameters: $\Theta = 1.3 \cdot 10^{-3}, \tau_A = 280$).

3 and 4 reproduces this behaviour. The agreement for the variance is quite satisfactory, for the mean value it is harder to judge, because of the strong fluctuations still present despite the averaging over 500 realisations.

3 A first model

The observation of the numerically generated trajectories reveals that the effect the noise has on the excitation are apparently random transitions of the configuration between basins of attraction corresponding to opposite signs of the propagation velocity. Also, only one absolute value of the velocity plays a role; there is no evidence of the involvement of other velocity values, which in priciple are possible in the system. We consider a countable set of possible velocity values v_i together with the probabilities $p_i(t)$ of the system being in the configuration corresponding to the propagation velocity v_i at time t. From the obvious relation

$$X(t) = \int_0^t v(t')\mathrm{d}t' \tag{5}$$

for the position $X(t)$ of the breather we obtain

$$\langle X(t) \rangle = \int_0^t \sum_i p_i(t') v_i \mathrm{d}t' = \sum_i v_i \int_0^t p_i(t')\mathrm{d}t' \tag{6}$$

for the mean value. For the two-time correlation function $C(t_2, t_1)$ we find

$$\begin{aligned} C(t_2,t_1) &:= \langle X(t_2)X(t_1)\rangle - \langle X(t_2)\rangle\langle X(t_1)\rangle = \\ &= \sum_{i,j} v_i v_j \int_0^{t_2}\int_0^{t_1} \left[p(v_i,t_2';v_j,t_1') - p_i(t_2')p_j(t_1')\right] \mathrm{d}t_1'\mathrm{d}t_2' = \\ &= \sum_{i,j} v_i v_j \int_0^{t_2}\int_0^{t_1} \left[p_{i|j}(t_2'|t_1') - p_i(t_2')\right] p_j(t_1')\mathrm{d}t_1'\mathrm{d}t_2' \end{aligned} \tag{7}$$

Herein $p(v_i, t_2'; v_j, t_1')$ is the joint probability of finding velocity v_i at time t_2' and velocity v_j at time t_1'; $p_{i|j}(t_2'|t_1')$ is the corresponding conditional probability $p_{i|j}(t_2'|t_1') = p(v_i, t_2'; v_j, t_1')/p_j(t_1')$. For the case of only two velocities $+v$ and $-v$ the above specialises to

$$\langle X(t)\rangle = v\left\{\int_0^t p_+(t')\mathrm{d}t' - \int_0^t \left[1-p_+(t')\right]\mathrm{d}t'\right\} = v\left[2\int_0^t p_+(t')\mathrm{d}t' - t\right], \tag{8}$$

as for only two values $p_- = 1 - p_+$, and

$$\begin{aligned} C(t_2,t_1) = v^2 \int_0^{t_2}\int_0^{t_1} \Big\{ &\left[p_{+|+}(t_2'|t_1') - p_+(t_2')\right] p_+(t_1') + \left[p_{-|-}(t_2'|t_1') - p_-(t_2')\right] p_-(t_1') \\ &- \left[p_{+|-}(t_2'|t_1') - p_+(t_2')\right] p_-(t_1') - \left[p_{-|+}(t_2'|t_1') - p_-(t_2')\right] p_+(t_1')\Big\} \mathrm{d}t_1'\mathrm{d}t_2' \end{aligned} \tag{9}$$

Up to now nothing has been said about the probabilities occuring in (8) and (9). We *assume* that there is a constant probability Θ per unit time for a change in the sign of the velocity. This leads to

$$\frac{\mathrm{d}p_+}{\mathrm{d}t} = \Theta(p_- - p_+) \tag{10}$$

$$\frac{\mathrm{d}p_-}{\mathrm{d}t} = \Theta(p_+ - p_-) \tag{11}$$

with the solutions

$$p_+(t) = \tfrac{1}{2} + \tfrac{1}{2}\left(p_+ - p_-\right)(0)\exp\left(-2\Theta t\right) \tag{12}$$

$$p_-(t) = \tfrac{1}{2} - \tfrac{1}{2}\left(p_+ - p_-\right)(0)\exp\left(-2\Theta t\right). \tag{13}$$

We furthermore find:

$$p_{+|-}(t_2'|t_1') = p_{-|+}(t_2'|t_1') = \tfrac{1}{2} - \tfrac{1}{2}\exp\left[-2\Theta\left(t_2' - t_1'\right)\right] \tag{14}$$

$$p_{+|+}(t_2'|t_1') = p_{-|-}(t_2'|t_1') = \tfrac{1}{2} + \tfrac{1}{2}\exp\left[-2\Theta\left(t_2' - t_1'\right)\right] \tag{15}$$

Choosing the initial condition to have positive sign of the velocity, from these expressions and (8),(9) we obtain

$$\langle X(t)\rangle = \frac{v}{2\Theta}\left[1 - \exp\left(-2\Theta t\right)\right], \qquad \lim_{t\to\infty}\langle X(t)\rangle = \frac{v}{2\Theta} \tag{16}$$

and

$$C(t_2,t_1) = \frac{v^2}{2\Theta^2}\left[1 - \exp(-2\Theta t_2)\right]\left[\cosh(2\Theta t_1) - 1\right] \tag{17}$$

From the latter expression we find for the variance of the position

$$Var\left[X(t)\right] = 2\frac{v^2}{\Theta^2}\exp(-\Theta t)\left[\sinh(\Theta t)\right]^3. \tag{18}$$

Asymptotically for long times, the variance behaves as $\exp(2\Theta t)$. This does not reflect the behaviour found in simulations. Thus, though due to the denominators of the prefactors in (16) and (18) an increase in the noise strength via an increase in Θ (this relation between Θ and σ is plausible and also evident from figure 1) reduces the mean value and partially has a suppressing effect on the variance, the results are not satisfactory and an improvement of the model is called for. The next section is dedicated to it.

4 An improved model

Individual trajectories obtained in numerics clearly show that the localised excitations change the sign of their propagation velocity under the influence of the noise. This change implies a change in the configuration of the breather, more precisely a transition from one basin of attraction to another. Such a transition, however, does not happen instantaneously. Rather, there will be a time span during which the configuration is not close to one of the attractors; the dynamics during this transition period may be quite involved and is not a subject of this paper. We attempt to roughly capture the effects of the non-instantaneousness of the transition by the introduction of a transition time τ_A, during which the velocity of the breather is 0, and during which no further transitions may be initiated. This means that if a transition from the $+v$ state is initiated at time $t = 0$, then the velocity of the localised mode immediately acquires the value 0, which it will retain up to $t = \tau_A$, when the velocity jumps to $-v$. In particular, we do not take into consideration 'failed' transitions, i.e. jumps of the velocity from $+v$ to 0 and back to $+v$. It is unclear whether taking into account such processes would improve the model; reality is much more complex and can involve all kinds of trajectories in velocity space. It certainly would increase the number of parameters and assumptions in the model; therefore we confine ourselves to the simple model where each initiated transition after time τ_A ends in the attractor corresponding to the opposite sign of the velocity. We keep the assumption of the previous section that there is a constant probabibility Θ per unit time for a transition to be initiated.

The introduction of the 'delay time' τ_A limits the maximum number m of jumps occuring in time t to $m = [t/\tau_A] + 1$, where $[x]$ denotes the integer part of x. If we consider a trajectory with n jumps up to time t (note that this implies $t \geq (n-1)\tau_A$), the jumps occuring at times $T_1, T_2, \ldots, T_n$, with $0 \leq T_1 \leq T_2 - \tau_A \leq \cdots \leq T_n - \tau_A$, we obtain for the distance traversed by the ILM:

$$\begin{aligned} X(t) = v\,[&T_1 - (T_2 - T_1 - \tau_A) + (T_3 - T_2 - \tau_A) - \ldots \\ &\cdots - \pi(n)(T_n - T_{n-1} - \tau_A) + \pi(n)(t - T_n - \tau_A)] = \\ &v\left[-2\sum_{k=1}^{n}\pi(k)T_k + \pi(n)t + \frac{1-\pi(n)}{2}\tau_A\right], \end{aligned} \tag{19}$$

where $\pi(n)$ is the parity of n, i.e. $\pi(n) = +1$ if n is even and $\pi(n) = -1$ if n is odd. The expression (19) holds if $T_n \leq t - \tau_A$; in the case $T_n > t - \tau_A$ we find

$$X(t) = v \left[-2 \sum_{k=1}^{n-1} \pi(k) T_k - \pi(n) T_n + \frac{1 + \pi(n)}{2} \tau_A \right], \tag{20}$$

because the excitation does not move after the n-th jump. The temporal probability density of n jumps occuring at the times $T_1, \ldots, T_n$ is in the case $T_n \leq t - \tau_A$:

$$p(T_n, \ldots, T_1) = \exp(-\Theta T_1) \Theta \exp[-\Theta(T_2 - T_1 - \tau_A)] \ldots$$
$$\ldots \exp[-\Theta(T_n - T_{n-1} - \tau_A)] \Theta \exp[-\Theta(t - T_n - \tau_A)] = \Theta^n \exp[-\Theta(t - n\tau_A)] \tag{21}$$

and analogously in the case $T_n > t - \tau_A$:

$$p(T_n, \ldots, T_1) = \Theta^n \exp[-\Theta(T_n - (n-1)\tau_A)]. \tag{22}$$

Using the equations (19-22) the mean value of $X(t)$ can be calculated as

$$\langle X(t) \rangle = S_0(t) + \sum_{n=1}^{m-1} [S_{1,n}(t) + S_{2,n}(t)] + S_{3,m}(t) \tag{23}$$

with

$$S_0(t) = vt \exp[-\Theta t] \tag{24}$$

corresponding to no jumps, and, using the step function H,

$$S_{1,n}(t) = H(t - n\tau_A) v \Theta^n \exp[-\Theta(t - n\tau_A)] \int_{(n-1)\tau_A}^{t-\tau_A} \mathrm{d}T_n \int_{(n-2)\tau_A}^{T_n - \tau_A} \mathrm{d}T_{n-1} \ldots$$
$$\ldots \int_{\tau_A}^{T_3 - \tau_A} \mathrm{d}T_2 \int_{0}^{T_2 - \tau_A} \mathrm{d}T_1 \left[-2 \sum_{k=1}^{n} \pi(k) T_k + \pi(n) t + \frac{1 - \pi(n)}{2} \tau_A \right], \tag{25}$$

$$S_{2,n}(t) = H(t - n\tau_A) v \Theta^n \int_{t-\tau_A}^{t} \mathrm{d}T_n \exp[-\Theta(T_n - (n-1)\tau_A)] \int_{(n-2)\tau_A}^{T_n - \tau_A} \mathrm{d}T_{n-1} \ldots$$
$$\ldots \int_{\tau_A}^{T_3 - \tau_A} \mathrm{d}T_2 \int_{0}^{T_2 - \tau_A} \mathrm{d}T_1 \left[-2 \sum_{k=1}^{n-1} \pi(k) T_k - \pi(n) T_n + \frac{1 + \pi(n)}{2} \tau_A \right], \tag{26}$$

and

$$S_{3,m} = H(t - (m-1)\tau_A) \left[1 - H(t - m\tau_A) \right] v \Theta^m \times$$
$$\times \int_{(m-1)\tau_A}^{t} \mathrm{d}T_m \exp[-\Theta(T_m - (m-1)\tau_A)] \int_{(m-2)\tau_A}^{T_m - \tau_A} \mathrm{d}T_{m-1} \ldots \int_{\tau_A}^{T_3 - \tau_A} \mathrm{d}T_2 \int_{0}^{T_2 - \tau_A} \mathrm{d}T_1 \times$$
$$\times \left[-2 \sum_{k=1}^{m-1} \pi(k) T_k - \pi(m) T_m + \frac{1 + \pi(m)}{2} \tau_A \right]. \tag{27}$$

Several expressions are useful in evaluating these quantities as well as others to be introduced below. They are gathered in an appendix. After some algebra we arrive at

$$S_{1,n}(t) = H(t-n\tau_A)\frac{1+\pi(n)}{2}\frac{v}{\Theta}\exp[-\Theta(t-n\tau_A)]\frac{[\Theta(t-n\tau_A)]^{n+1}}{(n+1)!} \tag{28}$$

$$S_{2,n} = H(t-n\tau_A)\frac{1-\pi(n)}{2}\frac{v}{\Theta}\exp[-\Theta(t-n\tau_A)]\times$$
$$\times\sum_{l=0}^{n}\frac{1}{(n-l)!}\left\{[\Theta(t-n\tau_A)]^{n-l}-[\Theta(t-(n-1)\tau_A)]^{n-l}\,\mathrm{e}^{-\Theta\tau_A}\right\} \tag{29}$$

$$S_{3,m} = H(t-(m-1)\tau_A)\left[1-H(t-m\tau_A)\right]\frac{1-\pi(m)}{2}\frac{v}{\Theta}\times$$
$$\times\left\{1-\exp\left[-\Theta(t-(m-1)\tau_A)\right]\sum_{l=0}^{m}\frac{[\Theta(t-(m-1)\tau_A)]^{m-l}}{(m-l)!}\right\} \tag{30}$$

The expressions for $S_{2,n}$ and $S_{3,m}$ are complicated because of the polynomials appearing; in all the cases $S_{1,n}$,$S_{2,n}$ and $S_{3,m}$, however, we clearly see the 'retardation' caused by the introduction of τ_A.
In a similar way, the expectation of $X(t)^2$ can be written as

$$\langle X(t)^2\rangle = Q_0(t)+\sum_{n=1}^{m-1}\left[Q_{1,n}(t)+Q_{2,n}(t)\right]+Q_{3,m}(t) \tag{31}$$

with

$$Q_0(t) = v^2t^2\exp(-\Theta t) \tag{32}$$

$$Q_{1,n}(t) = H(t-n\tau_A)\frac{v^2}{\Theta^2}\exp\left[-\Theta(t-n\tau_A)\right]\frac{[\Theta(t-n\tau_A)]^{n+2}}{(n+2)!}\times$$
$$\times\left[\frac{1+\pi(n)}{2}(n+2)+\frac{1-\pi(n)}{2}(n+1)\right] \tag{33}$$

$$Q_{2,n}(t) = H(t-n\tau_A)\frac{v^2}{\Theta^2}\exp\left[-\Theta(t-n\tau_A)\right]\sum_{k=0}^{n+1}\left\{[\Theta(t-n\tau_A)]^{n+1-k}\right.$$
$$\left.-[\Theta(t-(n-1)\tau_A)]^{n+1-k}\,\mathrm{e}^{-\Theta\tau_A}\right\}\times$$
$$\times\left[\frac{1+\pi(n)}{2}\frac{n}{(n+1-k)!}+\frac{1-\pi(n)}{2}\frac{n+1}{(n+1-k)!}\right] \tag{34}$$

$$Q_{3,m}(t) = H(t-(m-1)\tau_A)\left[1-H(t-m\tau_A)\right]\frac{v^2}{\Theta^2}\times$$
$$\times\left\{\left(1-\exp\left[-\Theta(t-(m-1)\tau_A)\right]\right)\left(\frac{1+\pi(m)}{2}m+\frac{1-\pi(m)}{2}(m+1)\right)\right.$$
$$-\sum_{k=0}^{m}\left[\Theta(t-(m-1)\tau_A)\right]^{m+1-k}\exp\left[-\Theta(t-(m-1)\tau_A)\right]\times$$
$$\left.\times\left[\frac{1+\pi(m)}{2}\frac{m}{(m+1-k)!}+\frac{1-\pi(m)}{2}\frac{m+1}{(m+1-k)!}\right]\right\}. \tag{35}$$

From these results we can of course obtain $Var[X(t)] = \langle X(t)^2\rangle - \langle X(t)\rangle^2$, but as the expressions shown above are already rather involved, we do not carry out this step explicitly. However, from the above results the mean and the variance can easily be plotted and compared with the results from simulations, as done in figure 2. The results from fits for values $5\cdot 10^{-5} \le \sigma \le 15\cdot 10^{-5}$ clearly show that τ_A decreases with increasing noise strength (roughly as $\tau_A \propto 1/(k_B T)$), whereas Θ increases strongly, approximately as $\Theta \propto \exp[-\mu/(k_B T)]$ with some constant μ. Due to the strong fluctuations, clearer results are not possible; therefore we also do not show graphs.
The behaviour for short times $t < \tau_A$, $\Theta t \ll 1$, can be obtained from $S_{3,1}$ and $Q_{3,1}$. We find

$$\langle X(t)\rangle = \frac{v}{\Theta}\left[1 - \exp\left(-\Theta t\right)\right] \approx \frac{v}{\Theta}\left[\Theta t - \frac{1}{2}\left(\Theta t\right)^2 \ldots\right] \tag{36}$$

and

$$Var[X(t)] = \frac{v^2}{\Theta^2}\left[1 - 2\Theta t \exp\left(-\Theta t\right) - \exp\left(-2\Theta t\right)\right] \approx \frac{1}{3}\frac{v^2}{\Theta^2}\left(\Theta t\right)^3. \tag{37}$$

A completely different approach, which we will therefore present in a separate publication, easily yields the long-time ($t \gg 1/\Theta$) behaviour. The results are $\langle X\rangle = v/(2\Theta)$, which agrees with the result from section 3 independently of τ_A and $Var[X(t)] = Dt + c$ with

$$D = \frac{v^2}{\Theta^2\left(\tau_A + \frac{1}{\Theta}\right)}, \quad c \approx -\frac{v^2}{2\Theta^2}. \tag{38}$$

Here, even in the case $\tau_A \to 0$, an agreement with the simpler model of the previous section, where the variance shows exponential behaviour, is not achieved.

5 Discussion and Outlook

As we have seen, the diffusive behaviour of an intrinsic localised mode in the damped-driven discrete sine-Gordon chain, when Gaussian white noise is coupled to the system to model the effects of temperature, is due to random transitions between attracting configurations of the system that correspond to opposite signs of the propagation velocity of the mode. In this paper we have developed a model that satisfactorily describes this diffusion process. At a preliminary stage, the model only uses the transition probability per unit time, Θ, as parameter. This approach is not sufficient; it is improved by the introduction of a second parameter, the delay time τ_A. Both parameters are determined from fits to the results from simulations. These fits show that with increasing temperature τ_A decreases and Θ increases. The long time behaviour for both models is the same for the expectation of the position of the intrinsic localised mode, but not for the variance of the position, not even in the case of vanishing delay time. This is due to a fundamental difference between the two approaches we have presented. In the one-parameter model we have only taken into account the probabilities of finding the configurations in one of the attracting states or the other. The two-parameter model, on the other hand, follows single trajectories through time and considers the probabilities for repeated jumps between the basins of attraction to occur in one and the same trajectory. The nonvanishing delay time, during which propagation of the excitation and further jumps are forbidden, also introduces a non-Markovian element in the diffusion process. The model does not make use of any specific characteristics of the system; it

only requires the existence of the attracting states and the possibility to excite transitions between these states by noise. The details of such a transition will, we suspect, be sensitive to the particular system, but in the model that we have presented in section 4 the details are 'hidden' in the delay time τ_A. Thus the origin of deviations between the prediction of the model and the result of simulations, which show in the transient period between the very early stages of the stochastic evolution and the long time diffusive regime, lies in the dynamics of the transition from one attractor to the other.
A first step in the development of a more detailed model would be a calculation of the parameters Θ and τ_A from the system parameters C, α, F, ω_0 and the noise strength σ. A further step would be to go beyond the simple picture of 'delayed jumps' that is at the heart of our model and to include the dynamics in full. The latter step then should also be able to describe the behaviour in the transient time regime.

Acknowledgements

MM and LV acknowledge support from the European Commission within the Research Training Network (RTN) LOCNET, contract HPRN-CT-1999-00163. LV also was partially supported by the Ministry of Science and Technology of Spain through grant BFM2002-02345.

Appendix

We list here several expressions that arise in the evaluation of the mean value of X and of X^2. M in the equations below is not to be confused with the maximum number of jumps m.

$$\int_{(M-2)\tau_A}^{T_M-\tau_A} \mathrm{d}T_{M-1} \int_{(M-3)\tau_A}^{T_{M-1}-\tau_A} \mathrm{d}T_{M-2} \ldots \int_{\tau_A}^{T_3-\tau_A} \mathrm{d}T_2 \int_{0}^{T_2-\tau_A} \mathrm{d}T_1 = \frac{[T_M-(M-1)\tau_A]^{M-1}}{(M-1)!} \tag{39}$$

For $1 \le k \le M-1$

$$\int_{(M-2)\tau_A}^{T_M-\tau_A} \mathrm{d}T_{M-1} \int_{(M-3)\tau_A}^{T_{M-1}-\tau_A} \mathrm{d}T_{M-2} \ldots \int_{\tau_A}^{T_3-\tau_A} \mathrm{d}T_2 \int_{0}^{T_2-\tau_A} \mathrm{d}T_1 T_k =$$
$$k\frac{[T_M-(M-1)\tau_A]^{M}}{M!} + (k-1)\tau_A\frac{[T_M-(M-1)\tau_A]^{M-1}}{(M-1)!} \tag{40}$$

$$\int_{(M-2)\tau_A}^{T_M-\tau_A} \mathrm{d}T_{M-1} \int_{(M-3)\tau_A}^{T_{M-1}-\tau_A} \mathrm{d}T_{M-2} \ldots \int_{\tau_A}^{T_3-\tau_A} \mathrm{d}T_2 \int_{0}^{T_2-\tau_A} \mathrm{d}T_1 T_k^2 =$$
$$k(k+1)\frac{[T_M-(M-1)\tau_A]^{M+1}}{(M+1)!} + 2\tau_A k(k-1)\frac{[T_M-(M-1)\tau_A]^{M}}{M!} +$$
$$(k-1)^2\tau_A^2\frac{[T_M-(M-1)\tau_A]^{M-1}}{(M-1)!} \tag{41}$$

For $1 \leq k < l \leq M-1$

$$\int_{(M-2)\tau_A}^{T_M-\tau_A} \mathrm{d}T_{M-1} \int_{(M-3)\tau_A}^{T_{M-1}-\tau_A} \mathrm{d}T_{M-2} \ldots \int_{\tau_A}^{T_3-\tau_A} \mathrm{d}T_2 \int_{0}^{T_2-\tau_A} \mathrm{d}T_1 T_k T_l =$$
$$(kl+k)\frac{[T_M-(M-1)\tau_A]^{M+1}}{(M+1)!} + (2kl-l-k)\tau_A \frac{[T_M-(M-1)\tau_A]^{M}}{M!} +$$
$$(kl-l-k+1)\tau_A^2 \frac{[T_M-(M-1)\tau_A]^{M-1}}{(M-1)!} \tag{42}$$

$$\sum_{k=1}^{n} \pi(k) = -\frac{1-\pi(n)}{2} \tag{43}$$

$$\sum_{k=1}^{n} \pi(k)k = \frac{1+\pi(n)}{2}\frac{n}{2} + \frac{1-\pi(n)}{2}\left(-\frac{n+1}{2}\right) \tag{44}$$

$$\sum_{l=k+1}^{n} \pi(l)l = \frac{1+\pi(n)}{2}\frac{n}{2} + \frac{1-\pi(n)}{2}\left(-\frac{n+1}{2}\right) -$$
$$\frac{1+\pi(k)}{2}\frac{k}{2} - \frac{1-\pi(k)}{2}\left(-\frac{k+1}{2}\right) \tag{45}$$

$$\sum_{k=1}^{n-1} \pi(k) \sum_{l=k+1}^{n} \pi(l)l = \frac{1+\pi(n)}{2}\left(-\frac{n^2}{4}-\frac{n}{2}\right) + \frac{1-\pi(n)}{2}\left(\frac{1}{4}-\frac{n^2}{4}\right) \tag{46}$$

$$\sum_{k=1}^{n-1} \pi(k) \sum_{l=k+1}^{n} \pi(l) = -\frac{1}{2}\frac{1+\pi(n)}{2} - \frac{1}{2}(n-1) \tag{47}$$

$$\sum_{k=1}^{n-1} \pi(k)k \sum_{l=k+1}^{n} \pi(l) = \frac{1-\pi(n)}{2}\left(-\frac{n^2}{4}+\frac{1}{4}\right) + \frac{1+\pi(n)}{2}(-\frac{n^2}{4}) \tag{48}$$

$$\sum_{k=1}^{n-1} \pi(k) \sum_{l=k+1}^{n} \pi(l)kl = \frac{1+\pi(n)}{2}\left(-\frac{n^3}{6}-\frac{n^2}{8}-\frac{n}{12}\right) +$$
$$\frac{1-\pi(n)}{2}\left(-\frac{n^3}{6}-\frac{n^2}{8}+\frac{n}{6}+\frac{1}{8}\right) \tag{49}$$

References

[1] Peyrard M 1998 *Physica* D **123** 403

[2] MacKay R S and Aubry S 1994 *Nonlinearity* **7** 1623

[3] Aubry S 1997 *Physica* D **103** 201

[4] Sepulchre J-A and MacKay R S 1997 *Nonlinearity* **10** 679

[5] Martínez P J, Meister M, Floría L M and Falo F 2003 *Chaos* to appear

[6] Sievers A J and Takeno S 1988 *Phys. Rev. Lett.* **61** 970

[7] Takeno S and Hori K 1990 *J. Phys. Soc. Japan* **59** 3037

[8] Cuevas J, Palmero F, Archilla J F R and Romero F R 2002 *J. Phys. A: Math. Gen.* **35** 10519

[9] Cuevas J, Palmero F, Archilla J F R and Romero F R 2002 *Phys. Lett.* A **299** 221

[10] Cuevas J, Archilla J F R, Gaididei Yu B and Romero F R 2002 *Physica* D **163** 106

[11] Pascual P J and Vázquez L 1985 *Phys. Rev.* B **32** 8305

[12] Rodríguez-Plaza M J and Vázquez L 1990 *Phys. Rev.* B **41** 11437

[13] Ivanov B A and Kolezhuk A K 1990 *Phys. Lett.* A **146** 190

[14] Quintero N R, Sánchez A and Mertens F G 1999 *Phys. Rev.* E **60** 222

[15] Quintero N R, Sánchez A and Mertens F G 2000 *Eur. Phys. J.* B **16** 361

[16] Meister M, Mertens F G and Sánchez A 2001 *Eur. Phys. J.* B **20** 405

[17] Ustinov A V 1998 *Physica* D **123** 315

[18] Marín J L, Falo F, Martínez P J and Floría L M 2001 *Phys. Rev.* E **63** 066603

[19] Gardiner C W 1985 *Handbook of Stochastic Methods* (Berlin: Springer)